Experimental investigation of the elastic enhancement factor in a microwave cavity emulating a chaotic scattering system with varying openness

Małgorzata Białous,[1] Barbara Dietz,[2,*] and Leszek Sirko[1,†]

[1]*Institute of Physics, Polish Academy of Sciences, Aleja Lotników 32/46, 02-668 Warszawa, Poland*

[2]*School of Physical Science and Technology, and Key Laboratory for Magnetism and Magnetic Materials of MOE, Lanzhou University, Lanzhou, Gansu 730000, China*

(Received 3 April 2019; published 18 July 2019)

A characteristic of chaotic scattering is the excess of elastic over inelastic scattering processes quantified by the elastic enhancement factor $F_M(T,\gamma)$, which depends on the number of open channels M, the average transmission coefficient T, and internal absorption γ. Using a microwave cavity with the shape of a chaotic quarter-bow-tie billiard, we study the elastic enhancement factor experimentally as a function of the openness, which is defined as the ratio of the Heisenberg time and the Weisskopf (dwell) time and is directly related to M and the size of internal absorption. In the experiments $2 \leqslant M \leqslant 9$ open channels with an average transmission coefficient $0.34 < T < 0.98$ and moderate internal absorption strength in the range of $\gamma = 0.9$–2.8 are achieved. The experimental results for the enhancement factor are shown to agree well with random matrix theory predictions. Furthermore, in order to corroborate the wave-chaotic features of the microwave system, the spectral fluctuation properties are studied for $M = 2$ channels. Agreement with those exhibited by typical, fully chaotic systems is illustrated, which is exemplary for the nearest-neighbor spacing distribution and the average power spectrum. Here we take into account the incompleteness of the sequence of resonance frequencies ascribed to the small yet nonvanishing internal absorption.

DOI: 10.1103/PhysRevE.100.012210

I. INTRODUCTION

The enhancement of elastic processes over inelastic ones in chaotic scattering was first detected in compound-nucleus cross sections [1,2] and also occurs in mesoscopic systems [3]. The elastic enhancement factor provides a measure for its size. It was introduced more than half a century ago by Moldauer [4] and since then has been considered as a probe of quantum chaos in nuclear physics [5–7] and other fields [8–11]. Within Hauser-Feshbach theory [12,13] the nuclear cross sections are expressed in terms of the scattering (S) matrix, of which the diagonal elements S_{aa} describe elastic processes and the off-diagonal ones S_{ba} inelastic ones, yielding for their energy average $\langle\sigma_{ba}^{\rm fl}\rangle = \langle|S_{ba}^{\rm fl}|^2\rangle$ and accordingly for the enhancement factor $F = \sqrt{\langle|S_{aa}^{\rm fl}|^2\rangle\langle|S_{bb}^{\rm fl}|^2\rangle}/\langle|S_{ba}^{\rm fl}|^2\rangle$. Using the equivalence of the scattering formalism for compound-nucleus reactions and for microwave resonators [14], properties of the elastic enhancement factor have been studied in such systems [10, 15–18] and also in microwave networks [19–21]. Investigations of aspects of quantum chaos in terms of the fluctuation properties of the scattering matrix associated with the measurement process are of particular interest from an experimental point of view because the latter are directly obtained in both the modulus and phase. Above all, large data ensembles may be attained and systems with preserved and also partially or completely violated time-reversal $\mathcal{T}$ invariance can be realized. A conjecture concerning the universality of the enhancement factor in electromagnetic fields in mode-stirred reverberating chambers was put forward by Fiachetti and Michelson [15] and has been further tested in wave scattering experiments with microwave cavities simulating quantum billiards [10,16] with a chaotic classical dynamics in the presence of absorption for the cases of preserved and partially violated $\mathcal{T}$ invariance. Quite recently, extensive studies of the elastic enhancement factor have been performed with microwave cavities with preserved $\mathcal{T}$ invariance in a low-absorption regime [17]. The reciprocal quantity $\Xi = 1/F$ was also considered both theoretically and experimentally in microwave cavities [16,17] and with microwave networks [22] simulating quantum graphs with preserved and violated $\mathcal{T}$ invariance in the presence of moderate and large absorption strength [19–21].

Experimentally, the S matrix is determined from measurements of resonance spectra, i.e., of ratios of the complex outgoing and incoming transmission or reflection amplitudes. The resonances acquire widths Γ which are composed of the width Γ_a due to absorption and the escape width $\Gamma_{\rm esc}$ due to additional open channels describing the coupling of the internal modes to the continuum. The coupling between the scattering channels c, which in our experiment correspond to antennas, and the interior region is quantified by the transmission coefficients $T_c = 1 - |\langle S_{cc}\rangle|^2$, where weak coupling $T_c \simeq 0$ corresponds to direct reflection back to the exterior without entering the scattering zone, whereas $T_c = 1$ implies perfect coupling. Furthermore, in our experiments the absorption is due to Ohmic losses in the walls of the microwave cavity. Its strength is related to Γ_a via $\gamma = \frac{2\pi\Gamma_a}{\Delta}$, where Δ denotes the average resonance spacing. For uniform

*dietz@lzu.edu.cn

†sirko@ifpan.edu.pl

Ohmic losses it can be modeled by means of a large number of weakly open fictitious channels [5,9]. In Ref. [7] the case of a large number M of weakly open channels with equal transmission coefficients T and no absorption was considered in terms of the openness $\eta = t_H/t_W = MT$. Here $t_H = 2\pi/\Delta$ is the Heisenberg time and $t_W = 1/\Gamma_{\rm esc}$ is the dwell time, i.e., the time an incoming microwave spends inside the cavity before it escapes through one of the M open channels like, e.g., an antenna [10]. The escape width can be expressed in terms of the Weisskopf width Γ_W, $\frac{2\pi}{\Delta}\Gamma_{\rm esc} = \frac{2\pi}{\Delta}\Gamma_W = MT$. In [11] an approximation was derived for the enhancement factor for the case of many weakly open channels with transmission coefficients $T_{\rm fict}$ and a few open channels with $T \gg T_{\rm fict}$. We realized such a situation experimentally in microwave experiments, where the weakly open channels correspond to the fictitious ones accounting for absorption. Accordingly, the enhancement factor $F_M(T,\gamma)$ depends on the absorption strength γ, the number of additional open channels M, and their average transmission coefficient T.

II. EXPERIMENT

Up to now, the enhancement factor $F_M(T,\gamma)$ has been studied experimentally only for the case of two open channels $M = 2$, even though the general case is of large relevance in nuclear physics and mesoscopic systems. We realized this case in microwave experiments performed with a flat cylindrical microwave cavity with the shape of a chaotic quarter-bow-tie billiard simulating a two-dimensional quantum billiard of corresponding shape [23–26]. Results were obtained for $2 \leqslant M \leqslant 9$ open channels and moderate internal absorption strength ranging from $\gamma = 0.90$ to 2.80 in the frequency range $\nu = 6$–12 GHz. Figure 1 shows a schematic view of the experimental setup. The cavity was constructed from two plates. A hole with the shape of the billiard was milled out of the bottom plate, whereas the top plate contained nine randomly distributed identical holes marked 1–9 in Fig. 1. The area of the hole equaled $A = 1828.5$ cm^2, the perimeter was $L = 202.3$ cm, and its height was $h = 1.2$ cm, corresponding to a cutoff frequency of $\nu_{\rm max} = c/2h \simeq 12.49$ GHz, with c the speed of light in vacuum. Above $\nu_{\rm max}$ the equivalence of the Helmholtz equation describing the microwave cavity and the Schrödinger equation for the corresponding quantum billiard no longer holds [23], whereas below $\nu_{\rm max}$ only the transverse magnetic modes can be excited inside the cavity so that the vectorial Helmholtz equation reduces to a scalar one. The top and bottom plates were squeezed together tightly with 127 screws at a distance of 2 cm. The cavity was manufactured from polished aluminum, type EN 5754. The whole inner surface of the cavity was covered by a 20-μm layer of silver so that the internal absorption was reduced by approximately 30% and a quality factor Q ranging from 2000 to 3000 was achieved.

The subunitary two-port scattering matrix $\hat{S}$,

$$\hat{S} = \begin{bmatrix} S_{11} & S_{12} \\ S_{21} & S_{22} \end{bmatrix}, \tag{1}$$

was measured with an Agilent E8364B microwave vector network analyzer which was coupled to the two measuring antennas at the positions marked 1 and 2 in Fig. 1 with

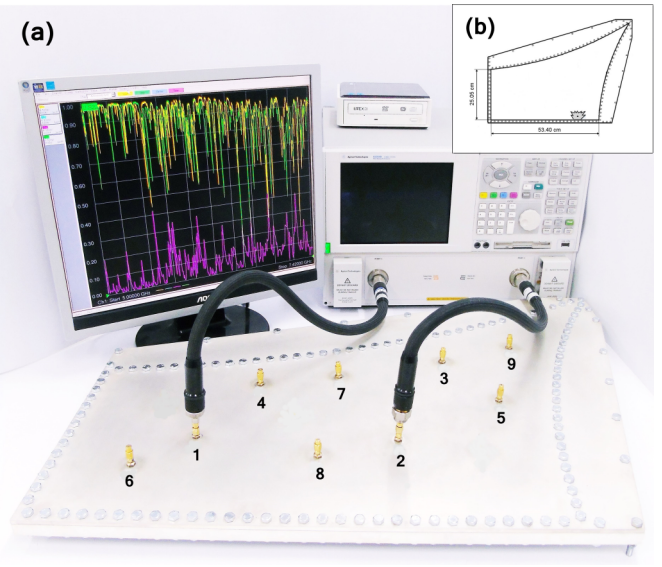

FIG. 1. (a) Photograph of the experimental setup. The measurements were performed with a vector network analyzer connected to the microwave antennas that protruded through the holes marked by 1 and 2 by flexible microwave cables. Additional open channels were realized by antennas with the same properties as the measuring ones but shunted with 50-Ω loads. (b) Schematic view of the quarter-bow-tie microwave cavity used for the measurement of the two-port scattering matrix $\hat{S}$. In order to realize an ensemble of differing cavities, a metallic perturber (gray) was moved along the wall of the cavity.

HP 85133-616 and HP 85133-617 flexible microwave cables. The antennas with pin diameter 0.9 mm and length 5.8 mm protruded through holes into the cavity and corresponded to two open channels. Additional open channels were realized by attaching additional antennas one by one with the same properties as the measuring ones to the holes according to their numbering but shunted with 50-Ω loads. A metallic perturber with area $A_{\rm pert} \simeq 9$ cm^2 and perimeter $L_{\rm pert} \simeq 26$ cm was inserted into the cavity and moved along the wall with an external magnet in order to create 100 different realizations of the cavity.

III. ANALYSIS OF RESONANCE SPECTRA

The elastic enhancement factor depends on the degree of $\mathcal{T}$ violation and is defined as

$$\begin{aligned} F_M^{(\beta)}(T,\gamma) &= \sqrt{\left\langle \left|S_{11}^{\rm fl}\right|^2 \right\rangle \left\langle \left|S_{22}^{\rm fl}\right|^2 \right\rangle} / \left\langle \left|S_{12}^{\rm fl}\right|^2 \right\rangle \\ &= \sqrt{C_{11}(0)C_{22}(0)}/C_{12}(0), \end{aligned} \tag{2}$$

with $\beta = 1$ for $\mathcal{T}$ invariant systems and $\beta = 2$ for completely violated $\mathcal{T}$ invariance,

$$S_{ab}(\nu) = \langle S_{ab} \rangle + S_{ab}^{\rm fl}(\nu) \tag{3}$$

with $a, b \in \{1, 2\}$, and $C_{ab}(0)$ denoting the S-matrix two-point correlation function

$$\begin{aligned} C_{ab}(\varepsilon) &= \langle S_{ab}(\nu) S_{ab}^*(\nu+\varepsilon) \rangle - |\langle S_{ab}(\nu) \rangle|^2 \\ &= \left\langle S_{ab}^{\rm fl}(\nu) S_{ab}^{\rm fl\,*}(\nu+\varepsilon) \right\rangle \end{aligned} \tag{4}$$

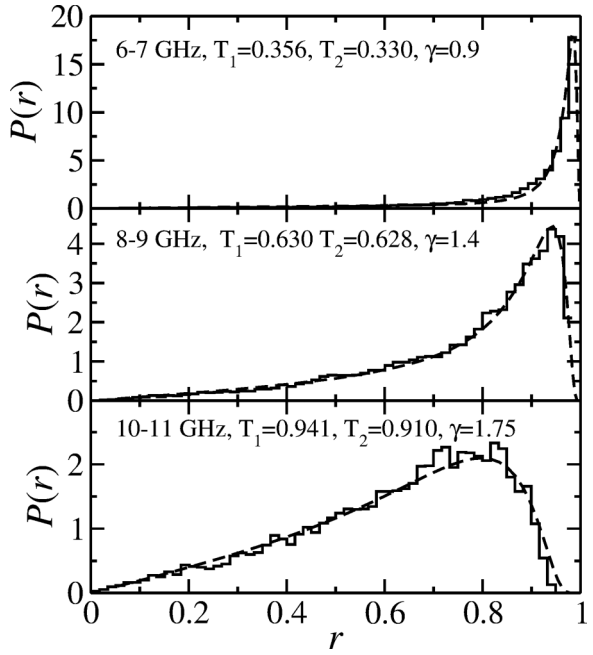

FIG. 2. Comparison of the experimental distributions (black histograms) of the reflection coefficients for the case of two open channels characterized by the transmission coefficients $T_1 \simeq T_2$ with the theoretical ones (black dashed lines). The frequency window and the values of T_1, T_2, and γ are given in the legends.

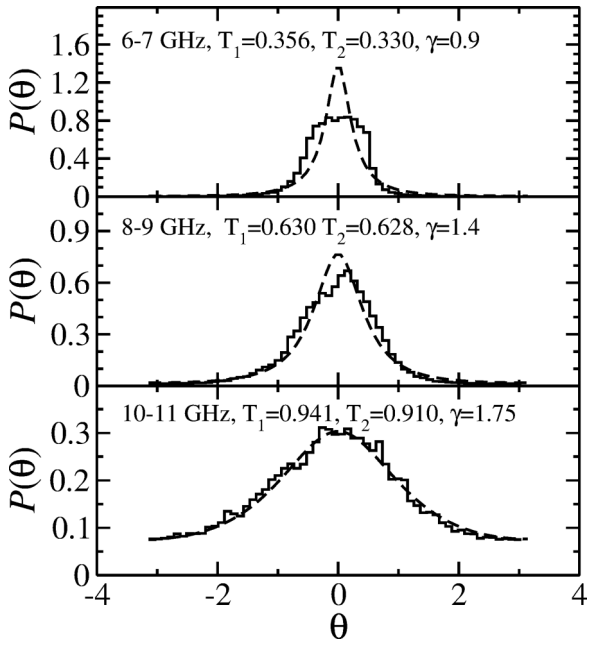

FIG. 3. Same as Fig. 2 for the scattering phases.

at $\epsilon = 0$. The S-matrix two-point correlation function and the enhancement factor depend on the values of the transmission coefficients T_c and on the absorption strength γ. In [6,8,27] exact analytical results were obtained for the two-point correlation function, and thus the enhancement factor, for preserved, violated, and also partially violated $\mathcal{T}$ invariance and tested thoroughly in [10]. In the limits of isolated resonances, yet a large number of weakly coupled channels, and of strongly overlapping ones, the enhancement factor approaches the values [8,9,11,16]

$$F_M^{(\beta)}(\{T_c\},\gamma) \to \begin{cases} 1+2/\beta & \text{for } \Gamma/\Delta \ll 1 \\ 2/\beta & \text{for } \Gamma/\Delta \gg 1. \end{cases} \quad (5)$$

In the present article we consider the case of $\mathcal{T}$ invariance, i.e., $\beta = 1$. Both the internal absorption γ in the walls of the cavity and the transmission coefficients describing the coupling of the antennas to the electric field modes inside the cavity depend on the microwave frequency. We checked that they are approximately constant in 1-GHz windows and accordingly evaluated them in such frequency intervals in the range from 6 to 12 GHz. Actually, absorption can be increased more effectively by the application of microwave absorbers. However, in the present article we are interested in the case of smallest possible absorption which can be controlled by the choice of the microwave frequency range.

The transmission coefficients are obtained from measurements of reflection spectra, $T_c = 1 - |\langle S_{cc}\rangle|^2$. For the determination of the absorption strength γ we considered $M = 2$ open channels, i.e., the case where just the two measuring antennas were attached to the cavity, and adjusted the theoretical distribution for the diagonal elements S_{aa} of the S matrix to the experimental ones. Here the index $a = 1, 2$ denotes the measuring-antenna ports. Using the notation

$$S_{aa} = \sqrt{r_a}e^{i\theta_a}, \quad x_a = \frac{1+r_a}{1-r_a}, \quad g_a = \frac{2}{T_a} - 1, \quad (6)$$

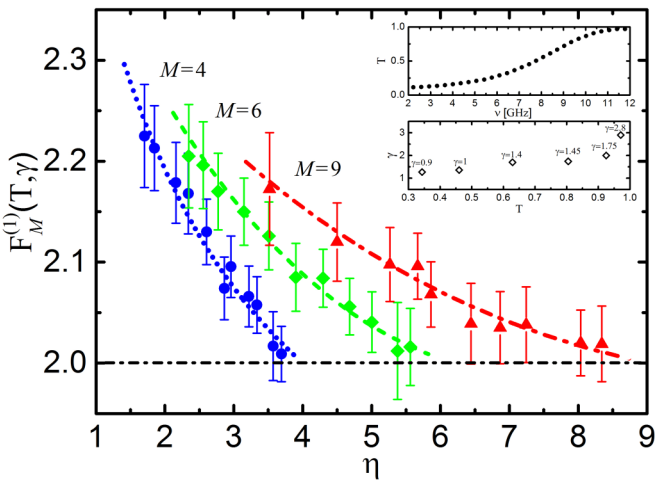

FIG. 4. Experimental elastic enhancement factor $F_M^{(1)}(T,\gamma)$, for $M = 4$ (blue circles), $M = 6$ (green diamonds), and $M = 9$ (red triangles), as a function of the openness η. The absorption strength γ changes from 0.9 to 2.8 for ν from 6 to 12 GHz. The theoretical results are shown as dotted lines with $M = 4$, 6, and 9 corresponding to blue, green, and red, respectively. The black dash-dotted line shows the random matrix theory limit of $F_M^{(1)}(T,\gamma)$ for strong absorption and/or large openness $\eta = MT$. The top inset shows the dependence of the average transmission coefficient T on the microwave frequency ν and the bottom the corresponding values of the absorption strength γ.

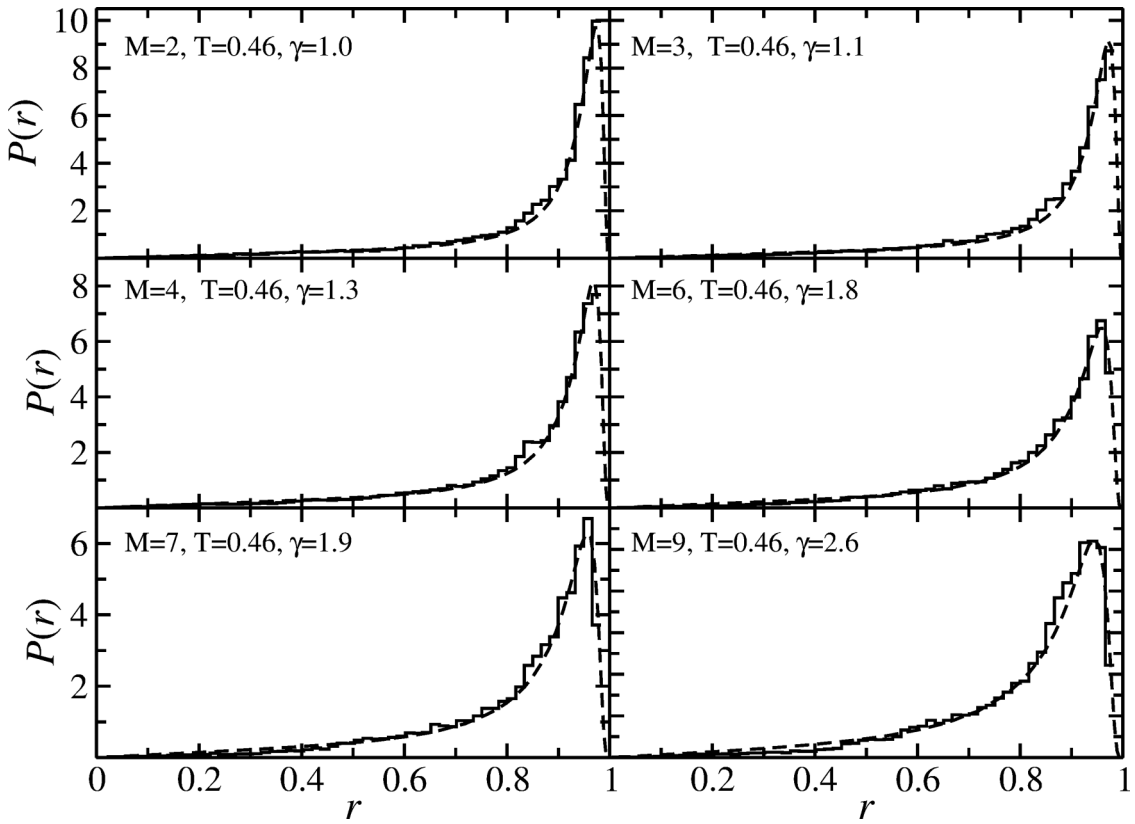

FIG. 5. Comparison of the experimental distributions (black histograms) of the reflection coefficients $P(r)$ for the case of M open channels with theory (black dashed lines) in the frequency window 7–8 GHz. The best agreement between the experimental result and theory was found when assuming two open channels for the antennas with average transmission coefficients T and accounting for the remaining open channels in the value for the absorption strength γ which is thus larger than in the case of two open channels (see Fig. 2). Accordingly, the average transmission coefficient due to these channels, i.e., their openness, seems to be smaller than that of the antennas. The value of T for the two antennas and of γ are given in the legends.

the distribution $P(x_a, \theta_a)$ of S_{aa} is obtained from

$$P(x_a,\theta_a)=\frac{1}{4\pi}\frac{d}{dy}(1+y)\Big[\gamma[K_1(w)J_2(w)+K_2(w)J_1(w)] + \sum_{c=1}^{M} t_c^a\big[L_1^c(w)H_2^c(w)+L_2^c(w)H_1^c(w)\big]\Big]\Big|_{y=y_a}, \tag{7}$$

with $y_a = x_a g_a + \sqrt{x_a^2-1}\sqrt{g_a^2-1}\cos\theta_a$, $w=\frac{y-1}{2}$, $t_c^a=1$ for $c=a$ and $t_c^a=T_c$ otherwise, and [8,10]

$$J_1(w)=\int_w^\infty dz\frac{e^{-\gamma z/2}}{\sqrt{z|z-w|}}\prod_{d=1}^{M}\frac{1}{\sqrt{1+t_d^a z}},$$

$$H_1^c(w)=\int_w^\infty dz\frac{e^{-\gamma z/2}}{\sqrt{z|z-w|}}\prod_{d=1}^{M}\frac{1}{\sqrt{1+t_d^a z}}\frac{1}{1+t_c^a z},$$

$$K_1(w)=\int_w^\infty dz\, e^{-\gamma z/2}\frac{\sqrt{z|z-w|}}{\prod_{d=1}^{M}\sqrt{1+t_d^a z}}\Big[\frac{e^{-\gamma}}{z+1}\prod_{d=1}^{M}\big(1-t_d^a\big) - \frac{1}{z}+\sum_{b=1}^{M}\frac{t_b^{a2}}{1+t_b^a z}\int_0^1 d\mu_0 e^{-\gamma\mu_0}\prod_{d\neq b}^{M}\big(1-t_d^a\mu_0\big)\Big],$$

$$L_1^c(w)=\int_w^\infty dz\, e^{-\gamma z/2}\frac{\sqrt{z|z-w|}}{\prod_{d=1}^{M}\sqrt{1+t_d^a z}}\Big[\frac{e^{-\gamma}}{z+1}\prod_{d\neq c}^{M}\big(1-t_d^a\big) - \frac{1}{z}+\sum_{b\neq c}\frac{t_b^{a2}}{1+t_b^a z}\int_0^1 d\mu_0 e^{-\gamma\mu_0}\prod_{d\neq b,c}^{M}\big(1-t_d^a\mu_0\big)\Big]. \tag{8}$$

In Figs. 2 and 3 we compare, for three frequency intervals, the experimental distributions of the reflection coefficients r_a, $P(r)\equiv P(r_a)$, and scattering phases θ_a, $P(\theta)\equiv P(\theta_a)$, for the case $M=2$ with the theoretical results obtained by integrating $P(x_a,\theta_a)$ over θ_a and r_a, respectively. The values of the frequency intervals, the transmission coefficients, and the absorption strength are given in the legends. The agreement between the experimental and theoretical curves is good above 8 GHz. This procedure yielded γ with a relative accuracy $\Delta\gamma/\gamma \simeq 0.06$. The results are shown in the insets of Fig. 4. In the presence of M open channels with average transmission coefficient T, corresponding to an openness $\eta = MT$ and internal absorption γ, the total rescaled width $\gamma^{\rm tot}=\frac{2\pi\Gamma}{\Delta}$ of the resonances is given by $\gamma^{\rm tot}=MT+\gamma$. Here we assume that the transmission coefficients associated with the two measuring antennas and those for the additional open channels

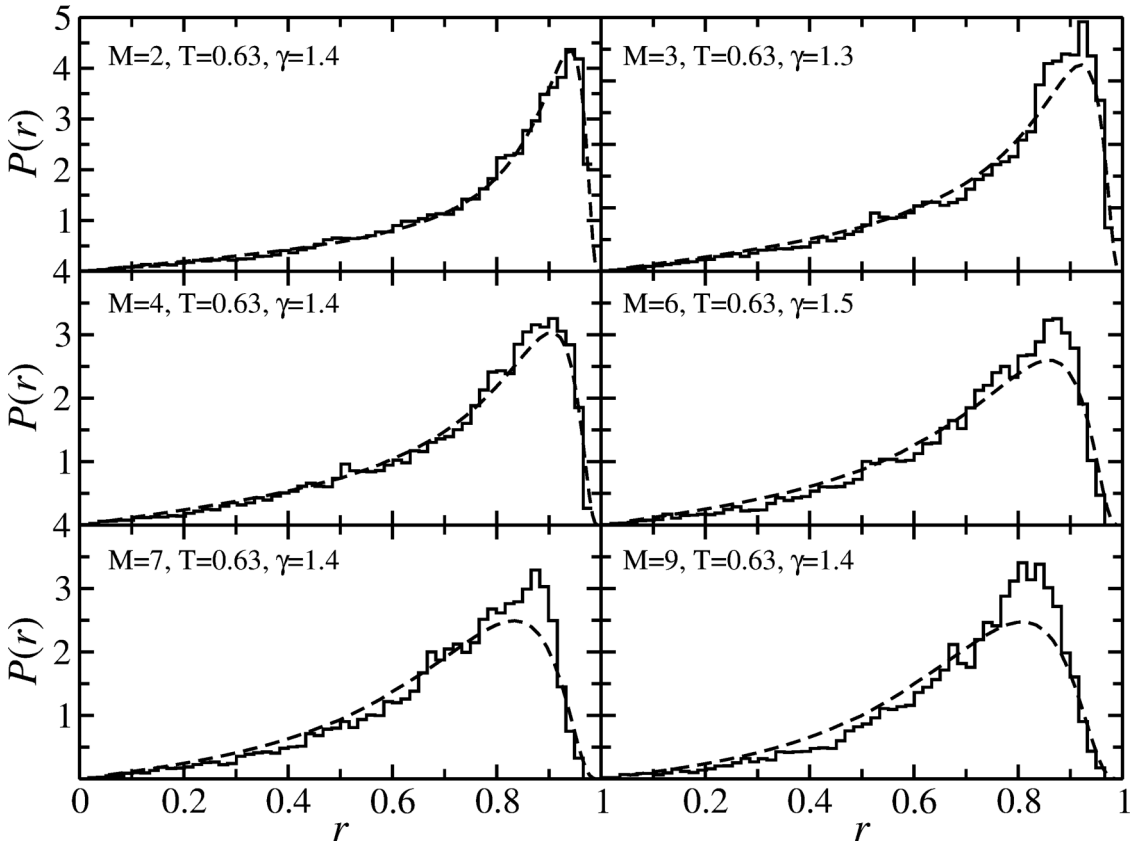

FIG. 6. Comparison of the experimental distributions (black histograms) of the reflection coefficients for the case of M open channels with theory (black dashed lines) in the frequency window 8–9 GHz. Good agreement was found when assuming that the transmission coefficients of two antennas and the remaining open channels are on average the same. The values of T and γ are given in the legends.

are approximately the same, which is justified because we chose antennas with equal properties and corroborated by the results for T_1 and T_2 (see Figs. 2 and 3). Accordingly, they are characterized by the average transmission coefficient $T = \frac{1}{M}\sum_{i=1}^{M} T_i$. These assumptions were carefully verified experimentally by adjusting the theoretical distributions for $M > 2$ to the experimental ones, yielding values for γ close to those obtained for the case $M = 2$ for $\nu \gtrsim 8$ GHz. Indeed, in the investigated frequency range $\nu = 6$–12 GHz all T_i were within 5% of each other. Below 8 GHz the experimental distributions for $M \geqslant 2$ attached antennas are better described by the theoretical ones for two open channels and an absorption larger than γ, i.e., there the effect of the additional open channels is to introduce absorption corresponding to an openness which is less than MT. Accordingly, the case $M > 2$ is achievable with our procedure for $\nu \gtrsim 8$ GHz (see Figs. 5 and 6).

The experimental results for $F_M^{(1)}(T,\gamma)$ were obtained in a sliding 1-GHz frequency window, which was shifted by 250 MHz between 6 and 12 GHz, and are shown to be exemplary for $M = 4$ (blue circles), $M = 6$ (green diamonds), and $M = 9$ (red triangles) in Fig. 4 as a function of the openness $\eta = MT$. Due to significant fluctuations of the enhancement factor $F_M^{(1)}(T,\gamma)$, which actually results from just one value ($\epsilon = 0$) of the S-matrix two-point correlation function (4), $F_M^{(1)}(T,\gamma)$ was obtained by averaging over the results for 100 different cavity realizations. The theoretical results for the enhancement factor were obtained from Eq. (4) by evaluating the exact analytical result for the S-matrix two-point correlation function [6] for M identical open channels. The absorption strength was modeled by $M_{\rm fict} = 50$ identical fictitious channels with the transmission coefficients $T_{\rm fict}$ set such that $\gamma = M_{\rm fict}T_{\rm fict}$. For the experimental values of total absorption $\gamma^{\rm tot} \leqslant 11.62$ and openness $\eta \leqslant 8.84$ we observe a clear dependence of $F_M^{(1)}(T,\gamma)$ on η, which follows well the theoretical curves, whereas for larger values it saturates at the value $F_M^{(1)}(T,\gamma) = 2$ corresponding to strong absorption and/or large openness (black dash-dotted line in Fig. 4). The top inset shows the average transmission coefficient as a function of frequency and the bottom one the corresponding values for the absorption strength γ.

IV. ANALYSIS OF SPECTRAL PROPERTIES

The spectral properties of generic quantum systems exhibiting a chaotic dynamics and preserved $\mathcal{T}$ invariance coincide with those of the eigenvalues of random matrices [28] from the Gaussian orthogonal ensemble (GOE) [29]. In order to corroborate that the quarter-bow-tie-shaped microwave cavity exhibits properties typical for quantum systems with classically chaotic counterparts, we furthermore analyzed the spectral fluctuation properties for the case of

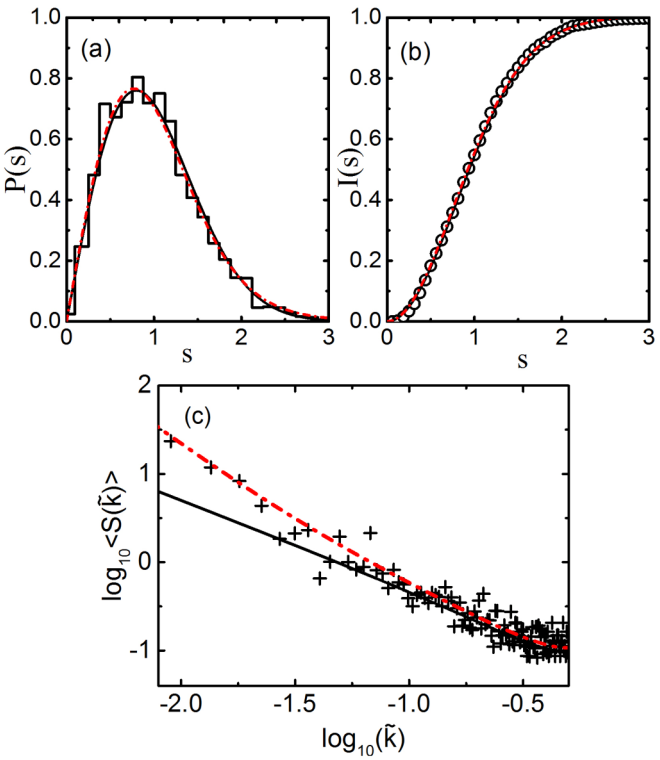

FIG. 7. (a) Nearest-neighbor spacing distribution $P(s)$ (histogram) for the case of two open channels $M = 2$ obtained in the frequency range 8–10 GHz. The experimental distribution is compared to the theoretical distribution (red dash-dotted line) accounting for randomly missing levels with the fraction of observed levels $\varphi = 0.94$ corresponding to 6% missing levels. The Wigner distribution for the GOE ($\varphi = 1$) is shown as a solid line. (b) Same as (a) for the integrated nearest-neighbor spacing distribution. The black circles show the experimental result. (c) Experimental average power spectrum $\langle s(\tilde{k})\rangle$ (black pluses) compared to the GOE results (red dash-dotted line) for a fraction of observed levels $\varphi = 0.94 \pm 0.01$ and $\varphi = 1$ (black solid line).

two open channels. Sequences of 200 resonance frequencies were determined in the frequency range from 8 to 10 GHz for 15 different realizations of the cavity and thereby an ensemble of 3000 levels was achieved. Comparison with Weyl's formula for two-dimensional microwave cavities revealed that approximately 6% of the resonance frequencies could not be identified. This is attributed to the absorption. Accordingly, we compared the experimental nearest-neighbor spacing distribution $P(s)$ to the Wigner distribution which provides a good approximation for that of the GOE and to the corresponding distribution which accounts for randomly missing levels [30,31] and depends on the fraction of observed levels φ. Furthermore, we analyzed the average power spectrum $\langle s(\tilde{k})\rangle$ [32]. The experimental distribution $P(s)$ for two open channels $M = 2$ is shown in Fig. 7(a) (histogram). It was averaged over the distributions for the 15 microwave cavity configurations. It agrees well with the nearest-neighbor spacing distribution (dash-dotted line) accounting for missing levels with $\varphi = 0.94$, corresponding to 6% missing levels, thus confirming the estimate based on Weyl's formula. Since the fraction of observed levels is close to 1, it is barely distinguishable from the Wigner distribution (solid line). Figure 7(b) shows the integrated nearest-neighbor spacing distribution $I(s)$ which has the advantage with respect to $P(s)$ that it does not depend on the binning.

Figure 7(c) shows the experimental result for the power spectrum (black pluses) of the deviation of the qth nearest-neighbor spacing from its mean value q, $\delta_q = \epsilon_{q+1} - \epsilon_1 - q$ [31–34]. For a sequence of N levels it is given in terms of the Fourier spectrum from "time" q to k, $S(k) = |\tilde{\delta}_k|^2$, with $\tilde{\delta}_k = \frac{1}{\sqrt{N}} \sum_{q=0}^{N-1} \delta_q \exp(-\frac{2\pi i k q}{N})$ and exhibits for $\tilde{k} = k/N \ll 1$ a power-law dependence $\langle S(\tilde{k})\rangle \propto (\tilde{k})^{-\alpha}$ [35,36]. For chaotic systems $\alpha = 1$, independently of whether $\mathcal{T}$ invariance is preserved or not, and for regular systems $\alpha = 2$. For the case of missing levels the power spectrum $\langle s(\tilde{k})\rangle$ is given by

$$\langle s(\tilde{k})\rangle = \frac{\varphi}{4\pi^2}\left[\frac{K(\varphi\tilde{k}) - 1}{\tilde{k}^2} + \frac{K(\varphi(1-\tilde{k})) - 1}{(1-\tilde{k})^2}\right] + \frac{1}{4\sin^2(\pi\tilde{k})} - \frac{\varphi^2}{12}. \quad (9)$$

Here $0 \leqslant \tilde{k} \leqslant 1$ and $K(\tau)$ denotes the spectral form factor which for $\tau \leqslant 1$ equals $K(\tau) = 2\tau - \tau\ln(1 + 2\tau)$ for the GOE. This measure is more sensitive to missing levels than the nearest-neighbor spacing distribution $P(s)$. The value of φ was unambiguously determined to $\varphi = 0.94 \pm 0.01$, by comparison of the experimental power spectrum to the theoretical one. Figure 7(c) shows the experimental result for $\langle s(\tilde{k})\rangle$ (black pluses) together with the theoretical one (red dash-dotted line). The experimental results are also compared to that for the GOE (black solid line). They agree well with the curve accounting for missing levels, thus confirming that we deal with a typical wave-chaotic system with a fraction of observed levels $\varphi = 0.94$.

V. CONCLUSION

In summary, we studied experimentally and numerically the elastic enhancement factor $F_M^{(1)}(T, \gamma)$ for a microwave cavity with the shape of a chaotic quarter-bow-tie billiard in the presence of open channels M characterized by an average transmission coefficient T and internal absorption γ as a function of the openness $\eta = MT$. The experimental results were obtained for $2 \leqslant M \leqslant 9$ open channels and moderate absorption strength $\gamma = 0.90$–2.80. We demonstrate that within the error in the determination of $F_M^{(1)}(T, \gamma)$ the experimental results are close to the theoretical predictions. Moreover, the spectral properties of the microwave cavity with $M = 2$ open channels were analyzed based on missing level statistics and illustrated for the nearest-neighbor spacing distribution and the average power spectrum. This analysis corroborated that the studied microwave cavity behaves like a typical chaotic system with preserved $\mathcal{T}$ invariance. These findings are crucial for the comparison of the experimental results with the theoretical ones which are based on random matrix theory. However, note that the fluctuation properties of the S matrix do not depend on missing resonances.

ACKNOWLEDGMENTS

This work was supported in part by the National Science Centre, Poland, Grants No. 2017/01/X/ST2/00734 and No. UMO-2016/23/B/ST2/03979, and the National Centre for Research and Development, Grant No. POIR.04.01.04-00-0144/17. B.D. thanks the National Natural Science Foundation of China for financial support through Grant No. 11775100.

[1] G. R. Satchler, Phys. Lett. **7**, 55 (1963).
[2] W. Kretschmer and M. Wangler, Phys. Rev. Lett. **41**, 1224 (1978).
[3] G. Bergmann, Phys. Rep. **107**, 1 (1984).
[4] Moldauer, Phys. Rev. **135**, B642 (1964).
[5] J. J. M. Verbaarschot, Ann. Phys. (N.Y.) **168**, 368 (1986).
[6] J. J. M. Verbaarschot, H. A. Weidenmüller, and M. R. Zirnbauer, Phys. Rep. **129**, 367 (1985).
[7] Y. Kharkov and V. Sokolov, Phys. Lett. B **718**, 1562 (2013).
[8] Y. V. Fyodorov, D. V. Savin, and H.-J. Sommers, J. Phys. A: Math. Gen. **38**, 10731 (2005).
[9] D. V. Savin, Y. V. Fyodorov, and H.-J. Sommers, Acta Phys. Pol. A **109**, 53 (2006).
[10] B. Dietz, T. Friedrich, H. L. Harney, M. Miski-Oglu, A. Richter, F. Schäfer, and H. A. Weidenmüller, Phys. Rev. E **81**, 036205 (2010).
[11] O. Zhirov and V. Sokolov, Acta Phys. Pol. A **128**, 990 (2015).
[12] W. Hauser and H. Feshbach, Phys. Rev. **87**, 366 (1952).
[13] H. M. Hofmann, J. Richert, J. W. Tepel, and H. A. Weidenmüller, Ann. Phys. (N.Y.) **90**, 403 (1975).
[14] S. Albeverio, F. Haake, P. Kurasov, M. Kuś, and P. Šeba, J. Math. Phys. **37**, 4888 (1996).
[15] C. Fiachetti and B. Michielsen, Electron. Lett. **39**, 1713 (2003).
[16] X. Zheng, S. Hemmady, T. M. Antonsen, Jr., S. M. Anlage, and E. Ott, Phys. Rev. E **73**, 046208 (2006).
[17] J.-H. Yeh, Z. Drikas, J. Gil Gil, S. Hong, B. T. Taddese, E. Ott, T. M. Antonsen, T. Andreadis, and S. M. Anlage, Acta Phys. Pol. A **124**, 1045 (2013).
[18] M. Ławniczak, M. Białous, V. Yunko, S. Bauch, and L. Sirko, Phys. Rev. E **91**, 032925 (2015).
[19] M. Ławniczak, S. Bauch, O. Hul, and L. Sirko, Phys. Rev. E **81**, 046204 (2010).
[20] M. Ławniczak, S. Bauch, O. Hul, and L. Sirko, Phys. Scr. **T143**, 014014 (2011).
[21] M. Ławniczak, S. Bauch, O. Hul, and L. Sirko, Phys. Scr. **T147**, 014018 (2012).
[22] O. Hul, S. Bauch, P. Pakoński, N. Savytskyy, K. Życzkowski, and L. Sirko, Phys. Rev. E **69**, 056205 (2004).
[23] H.-J. Stöckmann and J. Stein, Phys. Rev. Lett. **64**, 2215 (1990).
[24] S. Sridhar, Phys. Rev. Lett. **67**, 785 (1991).
[25] H.-D. Gräf, H. L. Harney, H. Lengeler, C. H. Lewenkopf, C. Rangacharyulu, A. Richter, P. Schardt, and H. A. Weidenmüller, Phys. Rev. Lett. **69**, 1296 (1992).
[26] L. Sirko, P. M. Koch, and R. Blümel, Phys. Rev. Lett. **78**, 2940 (1997).
[27] B. Dietz, T. Friedrich, H. L. Harney, M. Miski-Oglu, A. Richter, F. Schäfer, J. J. M. Verbaarschot, and H. A. Weidenmüller, Phys. Rev. Lett. **103**, 064101 (2009).
[28] M. L. Mehta, *Random Matrices* (Academic, London, 1990).
[29] O. Bohigas, M. J. Giannoni, and C. Schmit, Phys. Rev. Lett. **52**, 1 (1984).
[30] O. Bohigas and M. P. Pato, Phys. Lett. B **595**, 171 (2004).
[31] M. Ławniczak, M. Białous, V. Yunko, S. Bauch, and L. Sirko, Phys. Rev. E **98**, 012206 (2018).
[32] R. A. Molina, J. Retamosa, L. Muñoz, A. Relaño, and E. Faleiro, Phys. Lett. B **644**, 25 (2007).
[33] M. Białous, V. Yunko, S. Bauch, M. Ławniczak, B. Dietz, and L. Sirko, Phys. Rev. Lett. **117**, 144101 (2016).
[34] B. Dietz, V. Yunko, M. Białous, S. Bauch, M. Ławniczak, and L. Sirko, Phys. Rev. E **95**, 052202 (2017).
[35] A. Relaño, J. M. G. Gómez, R. A. Molina, J. Retamosa, and E. Faleiro, Phys. Rev. Lett. **89**, 244102 (2002).
[36] E. Faleiro, J. M. G. Gómez, R. A. Molina, L. Muñoz, A. Relaño, and J. Retamosa, Phys. Rev. Lett. **93**, 244101 (2004).